Far-Infrared Spectroscopy with SOFIA- the potential of GREAT

Helmut Wiesemeyer, Max-Planck-Institute for Radio Astronomy

SOFIA Tele Talk 2013 June 12

In collaboration with: R. Güsten, S. Heyminck, K. Jacobs, K.M. Menten, D. Neufeld, M.A: Requena-Torres, C. Risacher, J. Stutzki, F. Wyrowski

Historical context

[I was rather glad to find that my prejudice against meteoric matter was shared by others in the discussion on the lecture. One suggestion offered was molecular absorption. It is difficult to admit the existence of molecules in interstellar space because when once a molecule becomes dissociated there seems no chance of the atoms joining up again. The atoms will by ionisation lose their valency electrons and consequently lose their power of chemical combination; in fact the resulting positive charges will tend to hold them apart.

A.S. Eddington, 1926, Proc.Roy.Soc. Ser. A., 111, 424

Two somewhat stronger unidentified lines, whose sharpness indicates an interstellar character, have been detected at λ4232.6 and λ4300.3. The former is the stronger of the two. A third

T. Dunham, 1937, PASP 49, 26

this is rather unfavorable to the identification of CO_2. A search for the interstellar bands of CH, OH, NH, CN, and C_2 seems most interesting and promising. An interstellar line observed by Dunham[9] at λ 4300.3 may be due to CH. The only absorption lines of the

Swings & Rosenfeld, 1937, ApJ 86, 483

Survival of molecules in a harsh environment: dense knots exposed to strong UV radiation

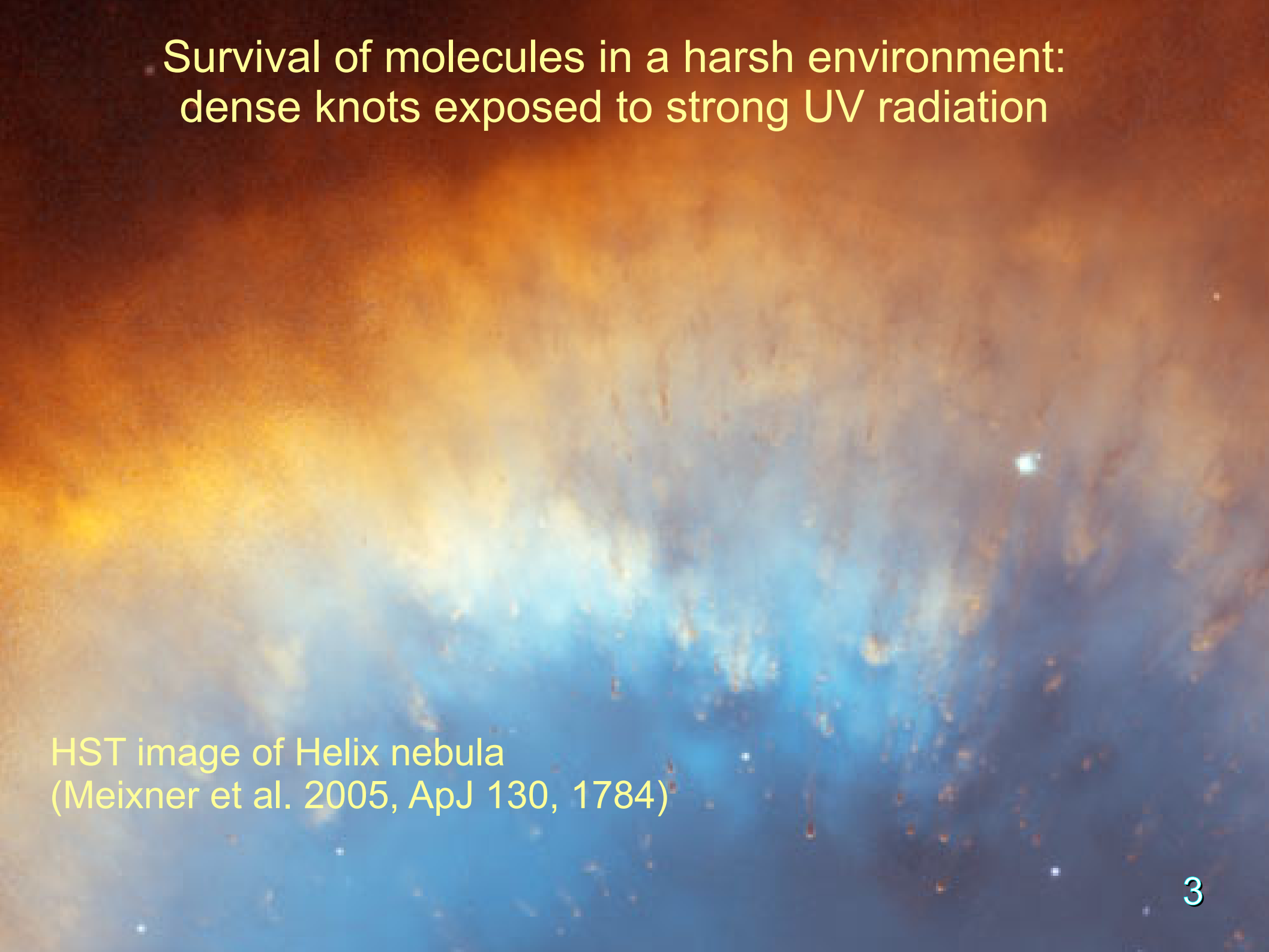

HST image of Helix nebula
(Meixner et al. 2005, ApJ 130, 1784)

Types of Interstellar Clouds

	Diffuse Atomic	Diffuse Molecular	Translucent	Dense Molecular
Defining Characteristic	$f^m_{H_2} < 0.1$	$f^m_{H_2} > 0.1$ $f^m_{C+} > 0.5$	$f^m_{C^+} < 0.5$ $f^m_{CO} < 0.9$	$f^m_{CO} > 0.9$
A_V (min.)	0	~0.2	~1-2	~5-10
Typical n_H [cm^{-3}]	10-100	100-500	500-5000 ?	$> 10^4$
Typical T [K]	30-100	30-100	15-50 ?	10-50
Observational Techniques	UV/Vis HI 21cm	UV/Vis IR abs mm abs	Vis (UV?) IR abs/em	IR abs mm em

Snow & Mc Call, 2006, ARA&A 44, 367

Phases of the ISM

Yorke 1988, Saas Fee Lecture

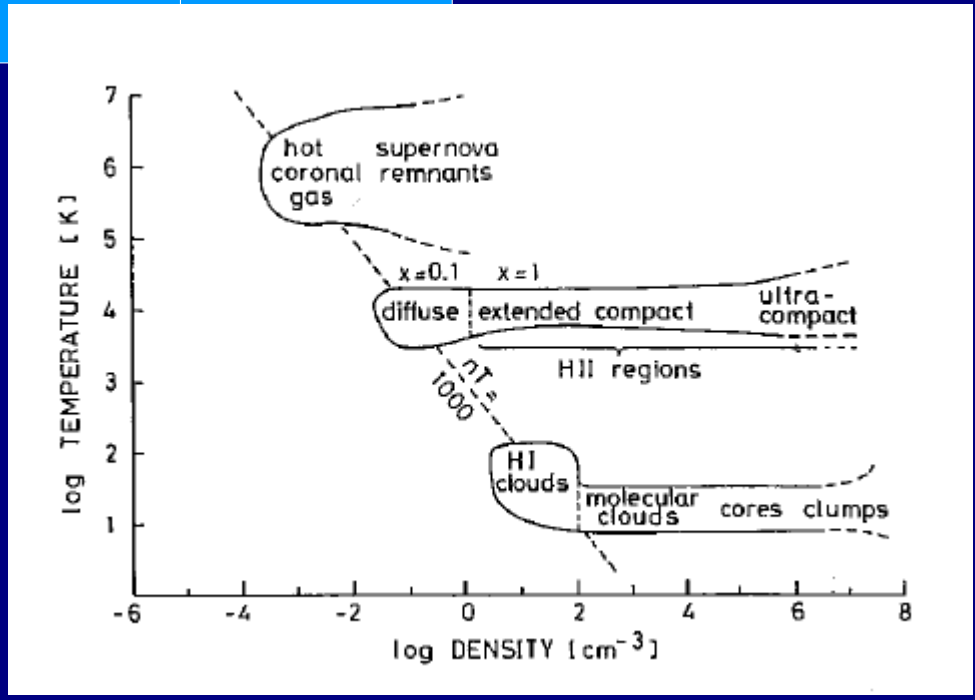

Chemistry of diffuse clouds

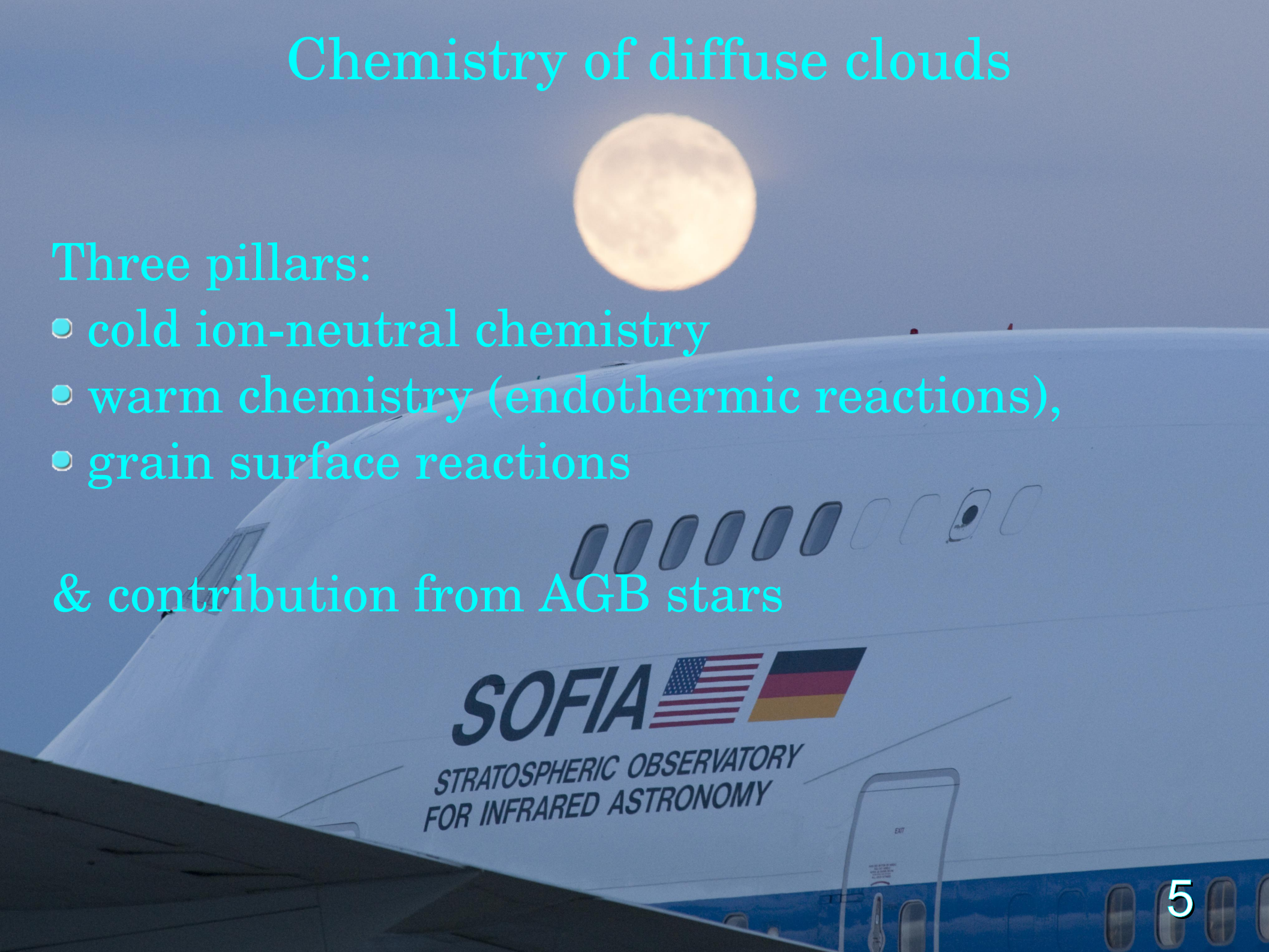

Three pillars:

- cold ion-neutral chemistry
- warm chemistry (endothermic reactions),
- grain surface reactions

& contribution from AGB stars

THz Spectroscopy with GREAT

Channel	Designation	Frequency Range [THz]	Lines of Interest
GREAT (single pixel)			
low-frequency	L1a	1.25-1.50	[NII], CO series, OD, HCN, H_2D^+
low-frequency	L1b	1.81-1.91	NH_3,OH($^2\Pi_{1/2}$),CO(16-15),[CII]
mid-frequency	Ma/b	2.5-2.7	OH($^2\Pi_{3/2}$), ^{18}OH, HD
high-frequency	H	4.7	[OI]
upGREAT (multi-beam)			
low-frequency array (14 pixels)	LFA	1.9-2.5	OH lines, [CII],CO series, [OI]
high-frequency array (7 pixels)	HFA	4.7	[OI]

Instantaneous bandwidth: 2.5 Ghz, highest spectral resolution 76.3 kHz
cf. Herschel/HIFI: Frequency range 480-1907 GHz,
230 MHz bandwidth at highest spectral resolution (130 kHz)

“Cold” Chemistry in the ISM

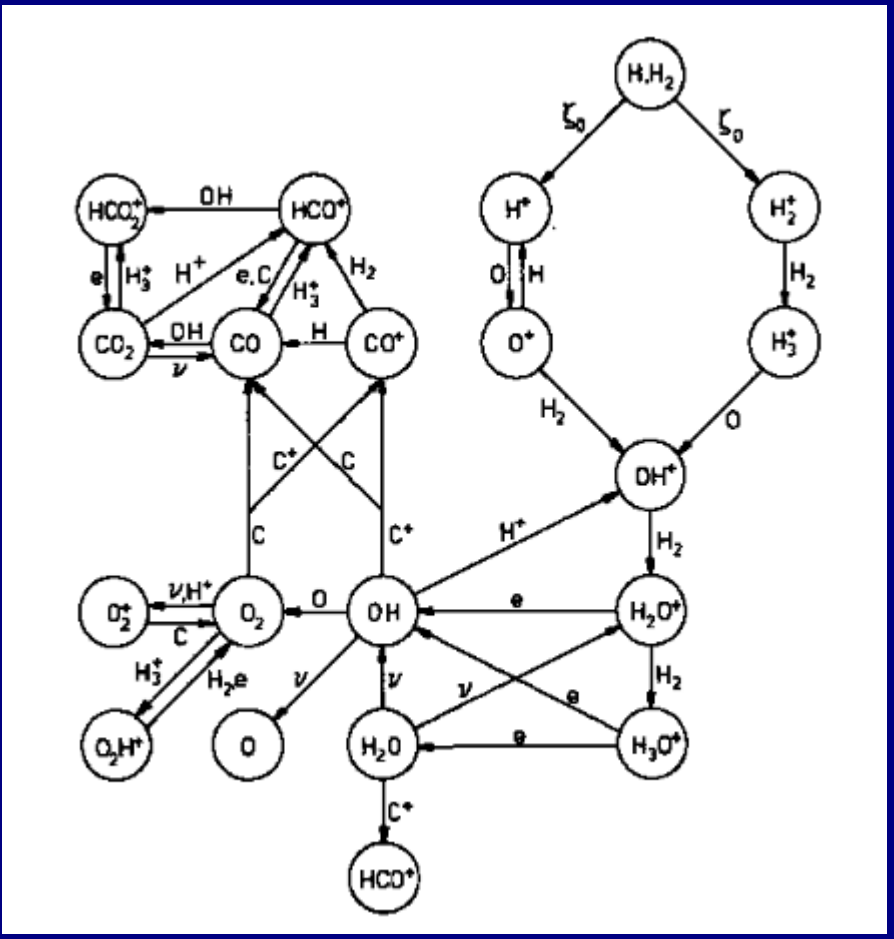

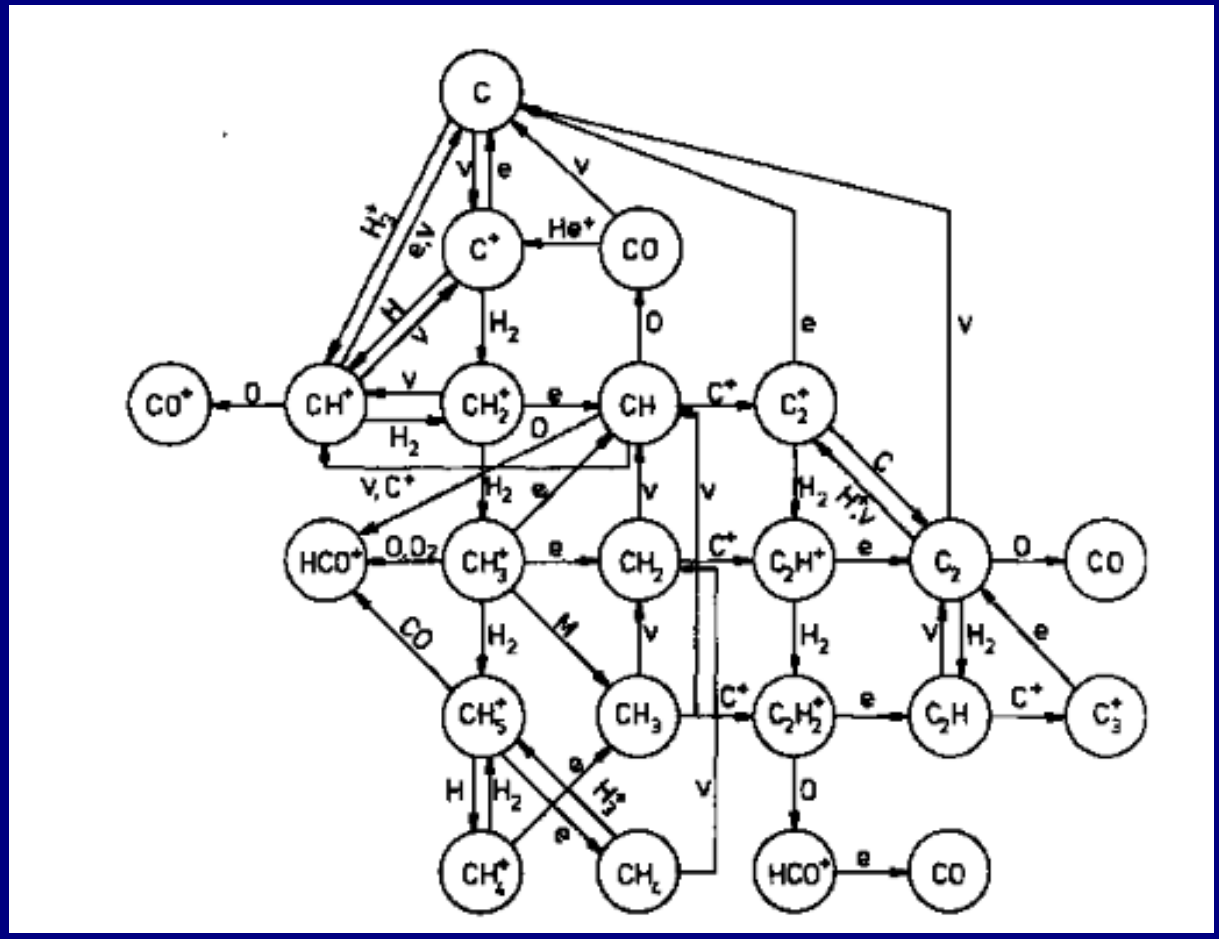

Reaction network for Oxygen bearing molecules

Reaction network for Carbon bearing molecules

(van Dishoeck & Black, 1986, ApJ 62, 109)

Ground state transitions of light hydrides

- HF as surrogate for H_2 (Neufeld & Wolfire 2009, Sonnentrucker et al. 2010)
- OH: column densities free from NLTE ambiguities

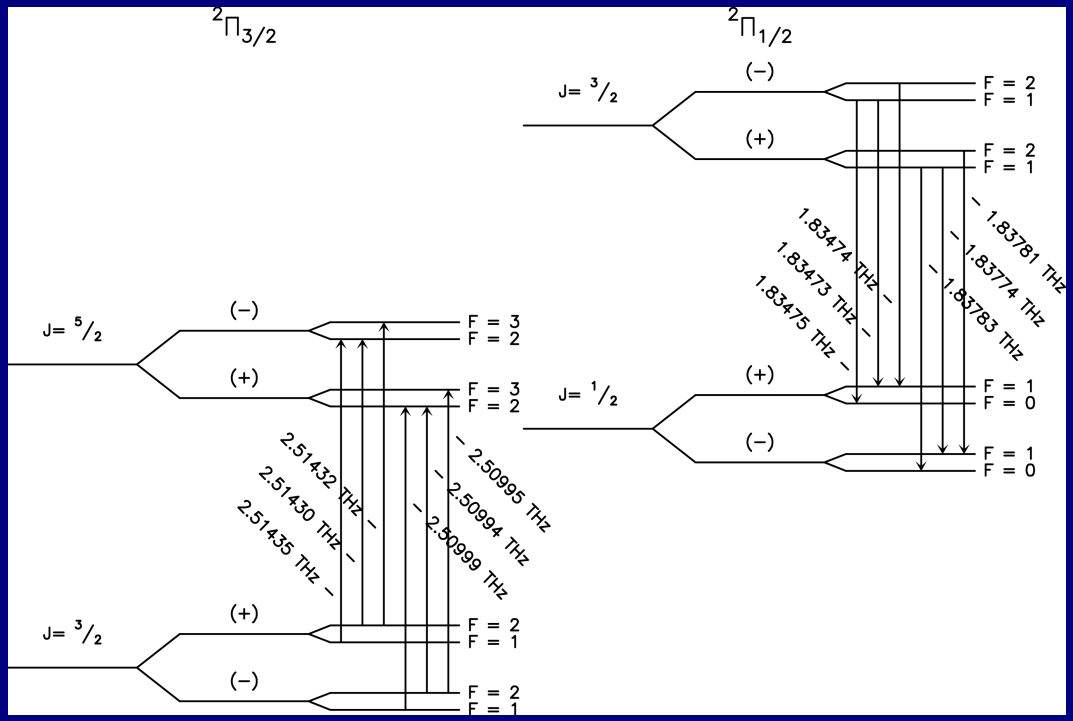

Level diagram for the OH $^2\Pi_{3/2}$ and $^2\Pi_{3/2}$ ground and first excited states

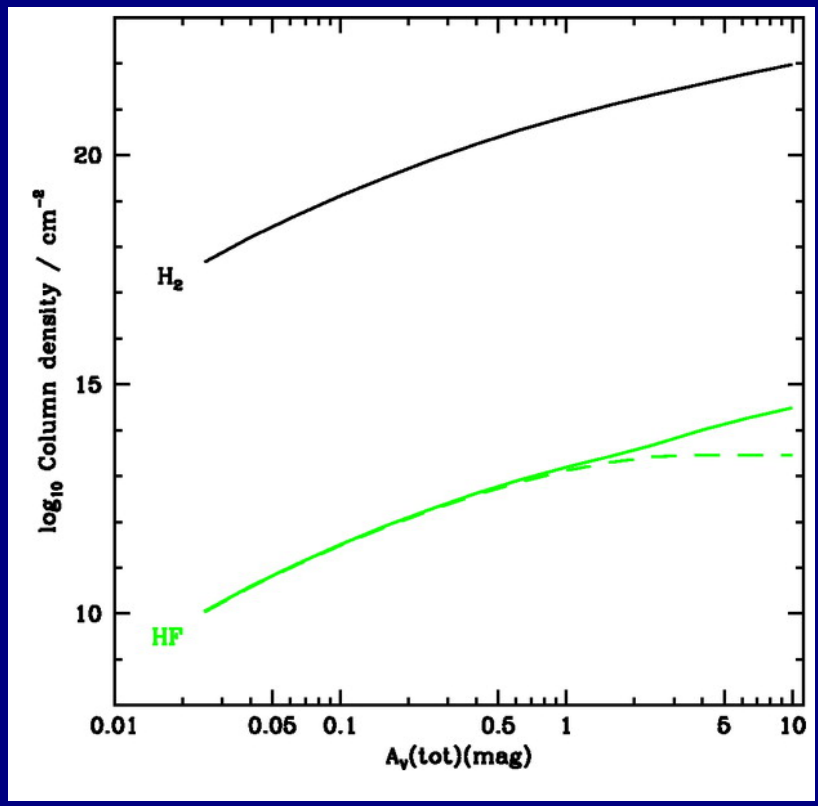

HF abundance in diffuse clouds (n_H = 100 cm^{-3}, X_{UV} = 1, Neufeld, Wolfire & Schilke 2005, ApJ 628, 260)

Radio observations of OH in diffuse clouds

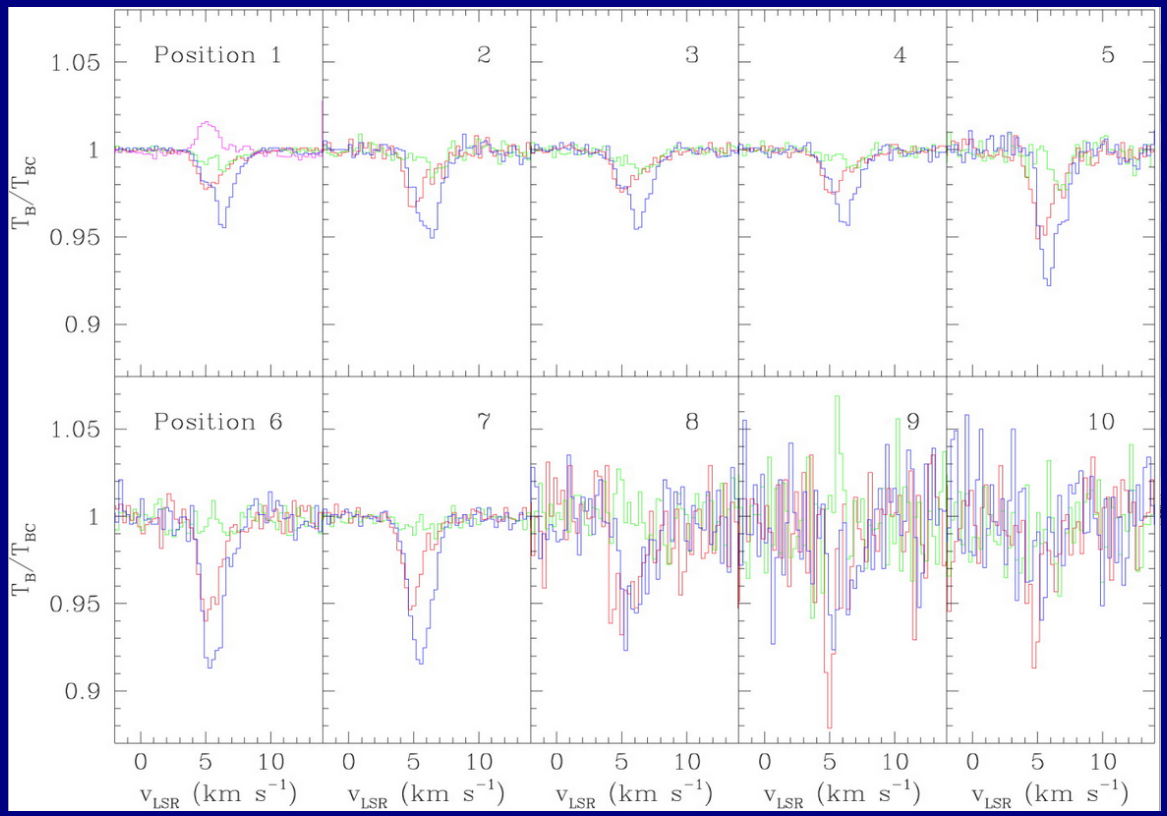

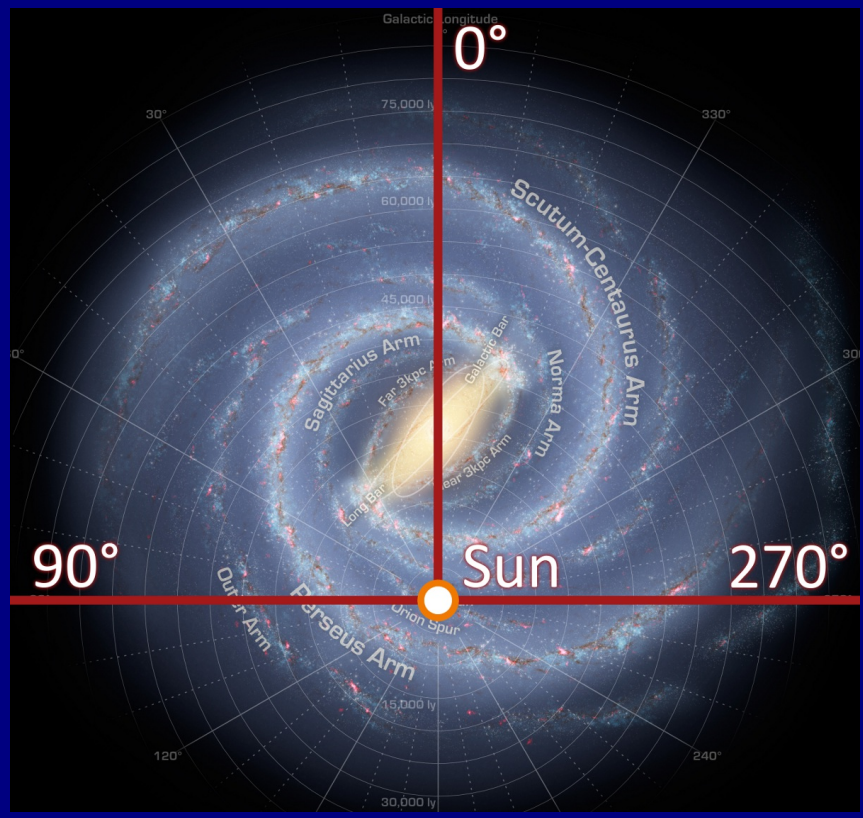

Neufeld et al. (2002): NLTE effects in OH HFS lines (W51, Arecibo data)

	Equivalent width ratios	
	observed	LTE
1612 MHz	2	1
1665 MHz	1	5
1667 MHz	3	9
1720 MHz	-1	1

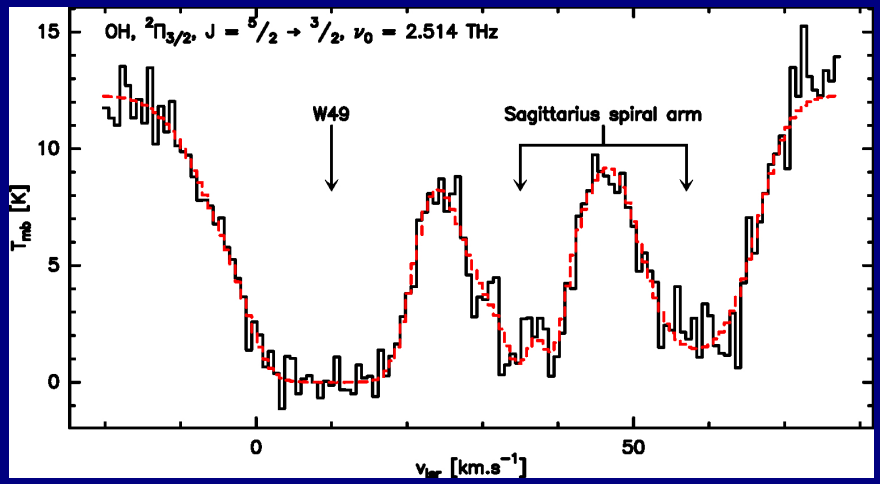

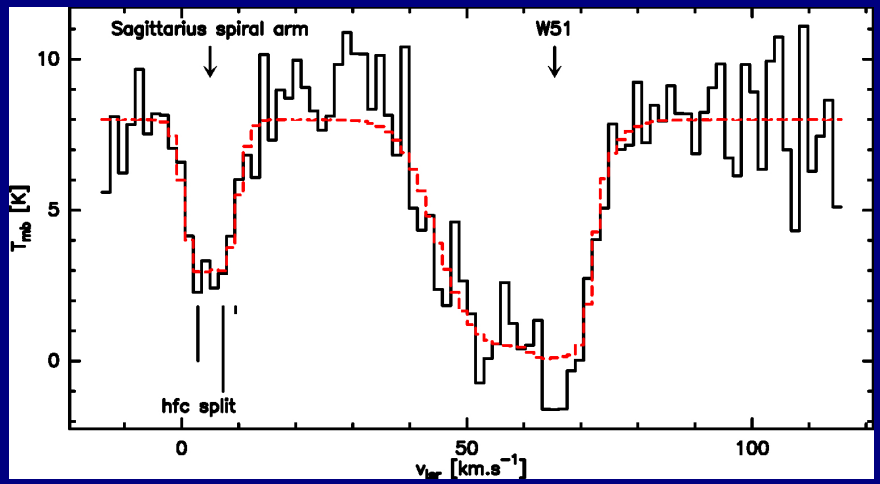

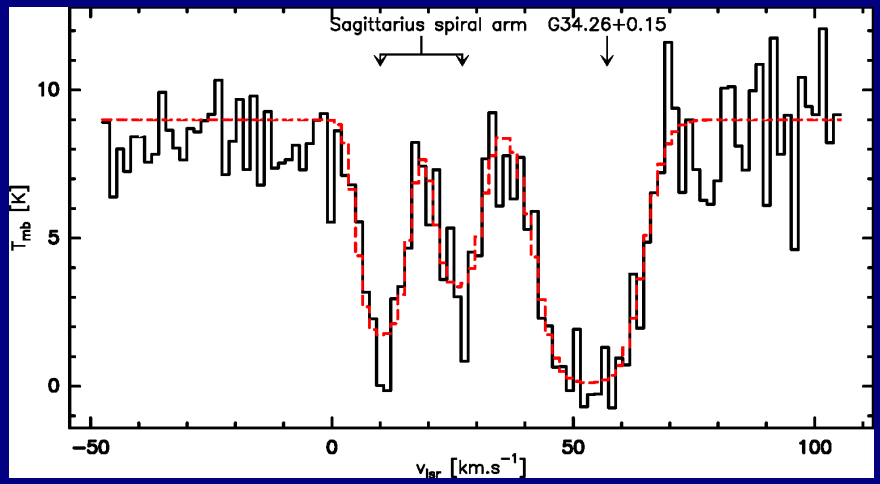

Wiesemeyer et al. 2012

- Absorption saturated towards continuum sources.
- KAO, ISO and PACS: spectral resolution insufficient, uniqueness of SOFIA/GREAT.
- Sight-line clouds: opacity substantial, but profile not saturated.
- Fit of Gaussian components: combined Metropolis/steepest descent method, convergence despite local minima:

$$\tau_{ij,\upsilon} = \sqrt{\frac{\ln 2}{\pi}} \frac{A_{E,j} c^3}{4\pi \Delta\upsilon_i \nu_j^3} \frac{g_{u,j}}{g_{1,j}} N_{OH} w_\Lambda \exp\left(-4 \ln 2 \left(\frac{\upsilon - \upsilon_{0,ij}}{\Delta\upsilon_i}\right)^2\right)$$

for each velocity & HF component.

- Error estimates from Monte-Carlo study.

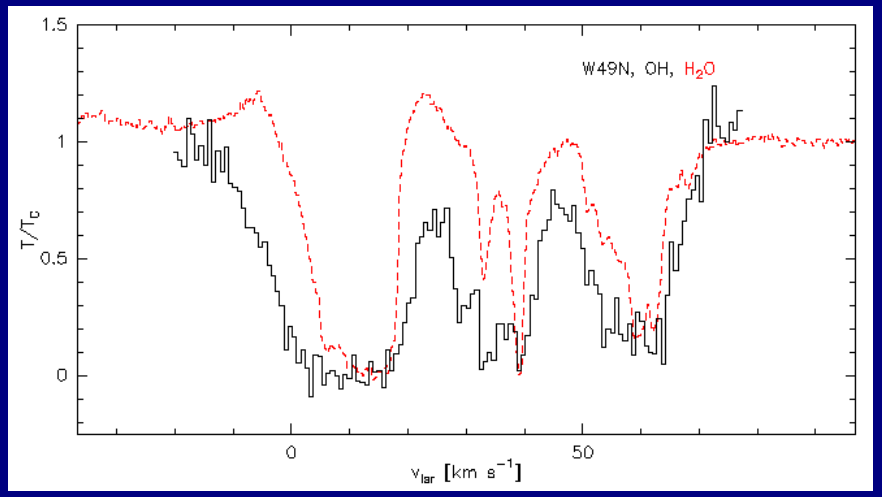

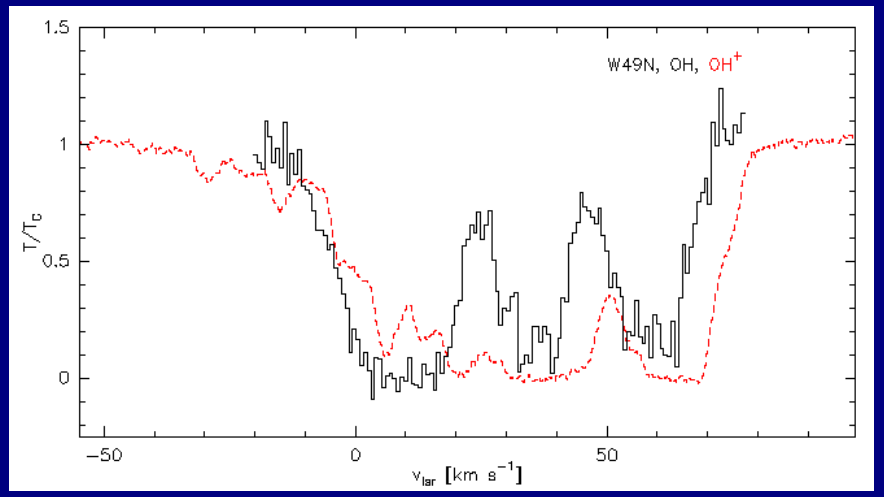

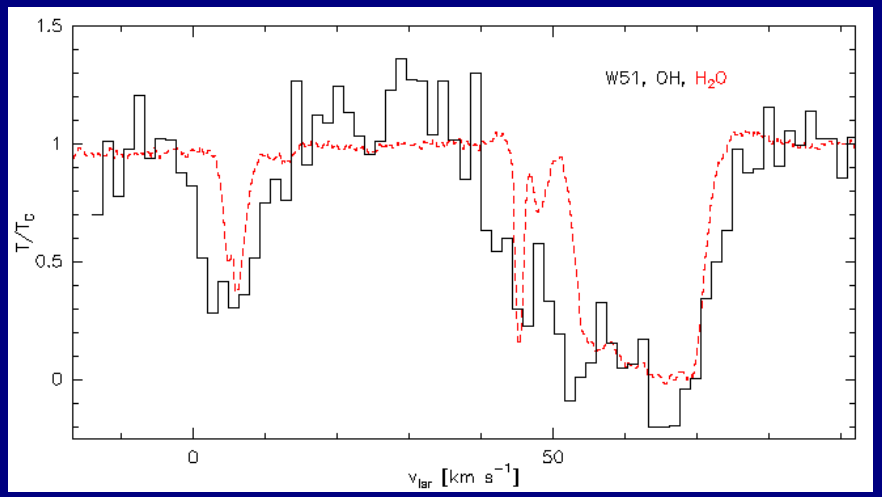

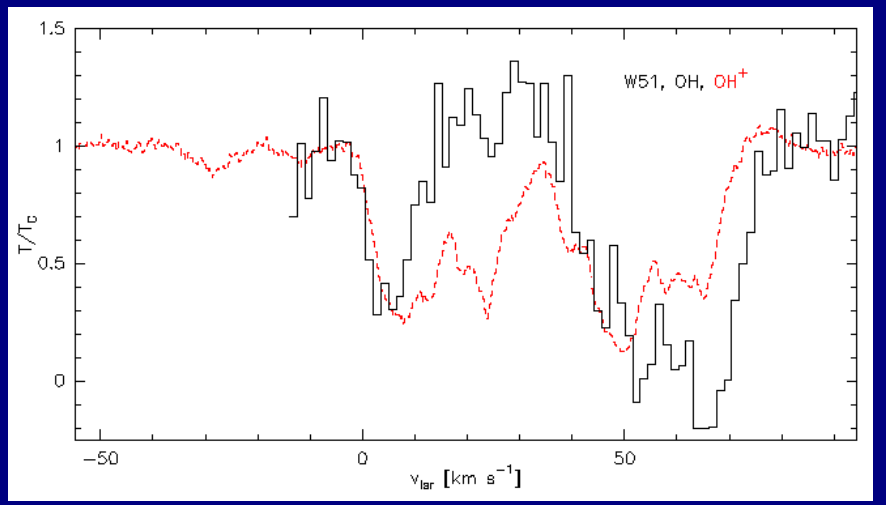

Observations need planning ahead:

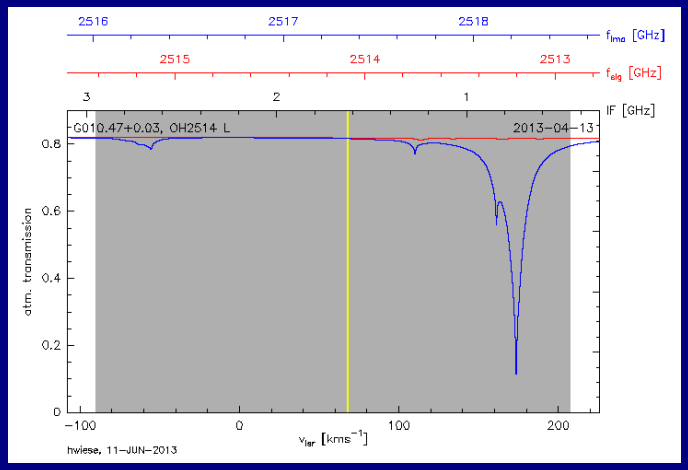

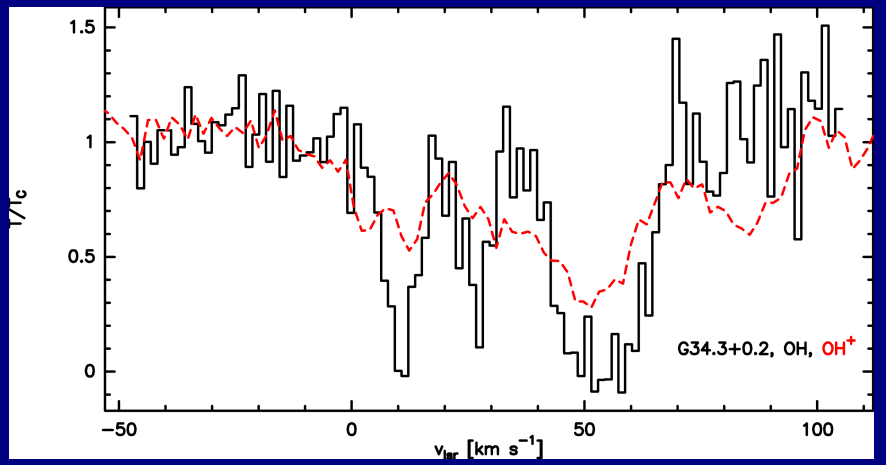

OH Formation through Cold, Ion-Neutral Chemistry

- Cosmic ray ionization of H or H_2, followed by
  $H_2^+(H_2,H)H_3^+(O,H_2)OH^+$ or $H^+(O,H)O^+(H_2,H)OH^+$
- Dissociation recombination of OH^+, or :
  $OH^+(H_2,H)H_2O^+(H_2,H)H_3O^+$
- Dissociation recombination of H_3O^+ to OH (~74% to 83 %) and H_2O (Jensen et al. 2000, Neau et al. 2000)
- Further OH formation by photo-dissociation of H_2O

OH Formation through Endothermic Pathway

$O(H_2,H)OH(H_2,H)H_2O$

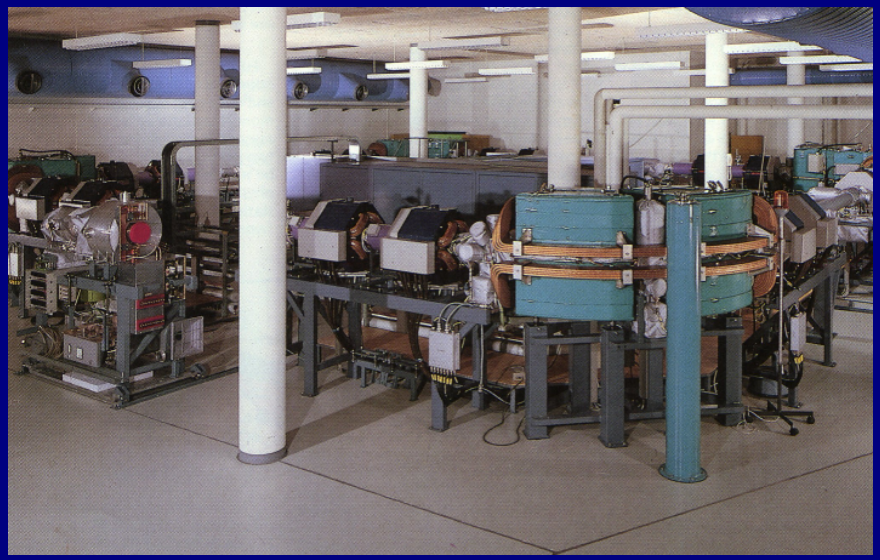

ASTRID Ion Storage Ring
(Aarhus, Denmark)

Table 3. OH and H_2O abundances and their ratios in line-of-sight clouds towards W49N and W51. Statistical errors are given in brackets.

		W49N v_{lsr} intervals [km s^{-1}]					W51 v_{lsr} intervals [km s^{-1}]		
		(30,37)	(37,44)	(44,49)	(49,54)	(54,72)	(−1,11)	(11,16)[c]	(43,50)
N_{OH}	[10^{13} cm^{-2}]	7.1(0.5)	11.3(6.3)	1.2(0.2)	1.5(0.3)	18.1(1.3)	6.4(0.9)	–	3.1(0.6)
$N^{(a)}_{H_2O}$	[10^{13} cm^{-2}]	2.3(0.1)	6.2(0.6)	0.1(0.05)	1.5(0.07)	11.6(0.4)	2.6(0.1)	0.23(0.05)	2.5(0.1)
$N^{(b)}_{H_2}$	[10^{20} cm^{-2}]	5.9(1.9)	6.6(2.0)	0.9(0.03)	3.2(0.1)	22.6(3.7)	4.3(0.1)	0.6(0.03)	2.6(0.8)
$[OH]/[H_2]$	[10^{-8}]	12.0(4.0)	17(11)	13.2(2.5)	4.5(0.9)	8.0(1.4)	15(2.1)	–	11.9(4.3)
$[H_2O]/[H_2]$	[10^{-8}]	3.9(1.3)	9.4(3.0)	1.1(0.6)	4.7(0.3)	5.1(0.9)	6.0(0.3)	3.8(0.9)	9.6(3.0)
$[H_2O]/[OH]$		0.32(0.03)	0.55(0.31)	0.08(0.04)	1.03(0.20)	0.64(0.05)	0.40(0.06)	–	0.81(0.16)

[a] Sonnentrucker (2010), [b] Godard et al. (2012). [c] The sensitivity of the OH observations is not sufficient for this velocity interval.

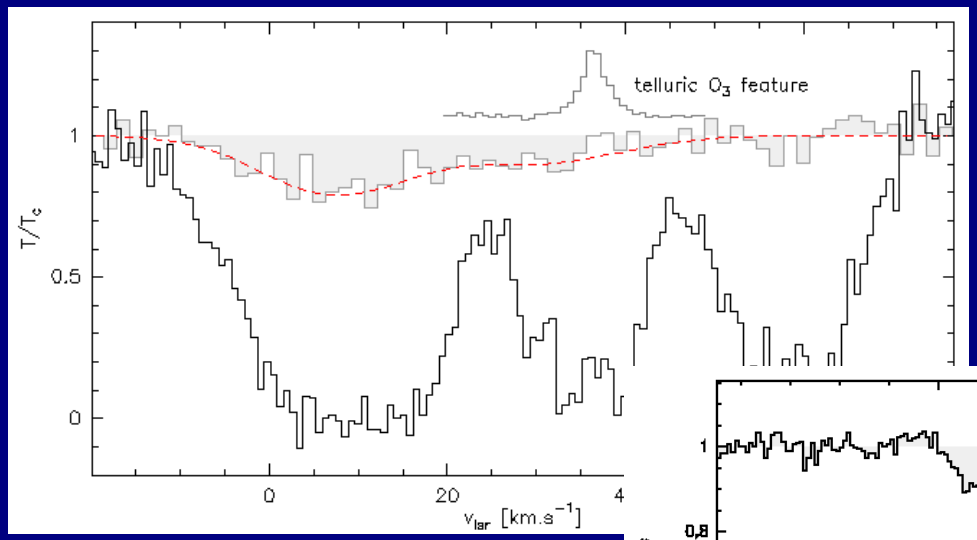

^{18}OH in W49N

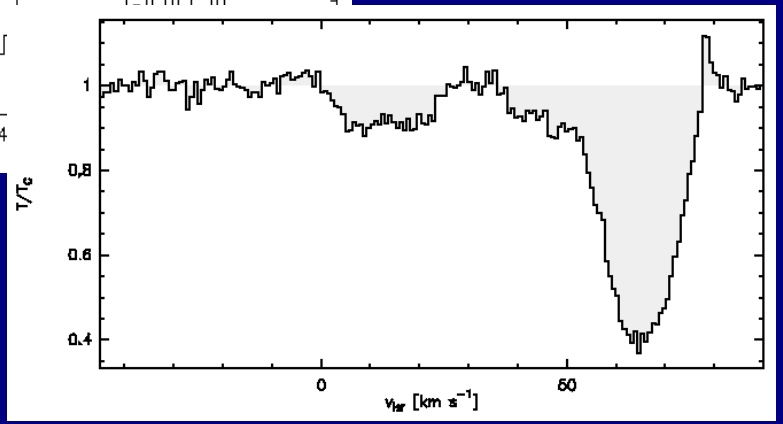

^{18}OH in SgrB2

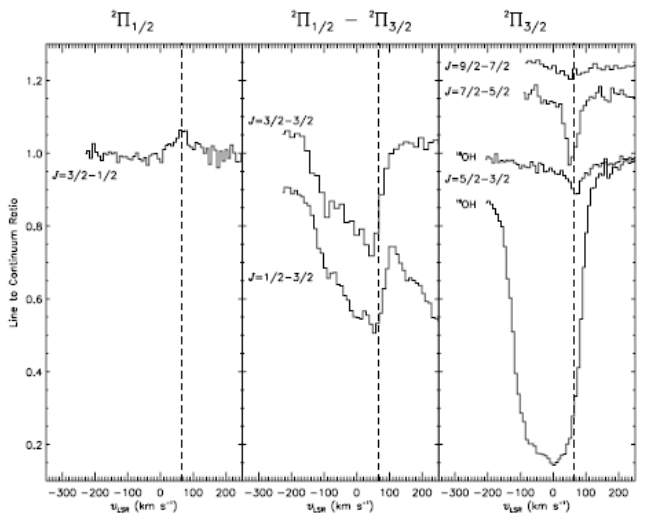

Figure 8. Observed rotational transitions of OH within and between the $^2\Pi_{1/2}$ and $^2\Pi_{3/2}$ ladders. The ground state line in the $^2\Pi_{3/2}$ ladder is shown for both ^{16}OH and ^{18}OH. The dashed line shows the velocity of Sgr B2 itself (65 km s^{-1}).

Polehampton et al. (2007)

The role of turbulent dissipation regions, TDRs

- Discovery of SH (Neufeld et al. 2012) and of its cation, SH^+ (Menten et al. 2011), in diffuse clouds,
- endothermic reactions enhanced in turbulent dissipation regions and slow shocks (no exothermic abstraction reactions, cf. CH^+, Falgarone et al. 2013).
- UV driven chemistry does not explain observed abundances, need non-equilibrium chemistry, Godard et al. 2009:
- Turbulence dissipated by ion-neutral friction (~100 AU shear structures).
- Application of techniques for molecular clouds ? Linewidth studies (Li & Houde 2008, Hezareh et al. 2010) & Chandrasekhar-Fermi method (Hildebrand et al. 2009)

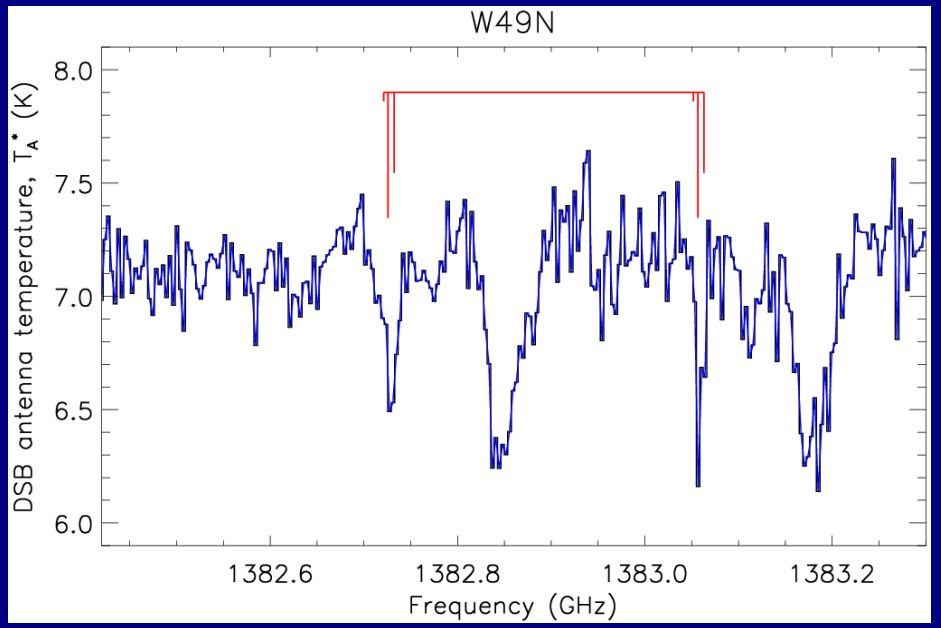

Neufeld et al. 2012, A&A 542, L6

Conclusions & Outlook

- First spectrally resolved observations of OH ground state absorption in diffuse clouds seen towards hot cores.
- Reliable OH column density determination.
- Confirmation of earlier column density estimates under NLTE.
- H_2O / OH = 0.3 – 1.0, lower end does not rule out TDRs.
- Correlation between OH and H_2O, but OH and OH^+ tend to be anti-correlated.
- ^{18}OH detection in Sgr B2 and, tentatively, W49N
- Long-term objective: role of endothermic gas phase reactions, grain surface chemistry, abundance gradients, rescale decades of radio column densities.
- Phases of the ISM: cloud concatenation vs. onion structure.


Thank you.
SOFIA
STRATOSPHERIC OBSERVATORY
FOR INFRARED ASTRONOMY
EXIT